



HAL
open science

The relationship between morphological lesion, magnetic source imaging, and intracranial stereo-electroencephalography in focal cortical dysplasia

Romain Bouet, François Mauguière, Sébastien Daligault, Jean Isnard, Marc Guenot, Olivier Bertrand, Julien Jung

► To cite this version:

Romain Bouet, François Mauguière, Sébastien Daligault, Jean Isnard, Marc Guenot, et al.. The relationship between morphological lesion, magnetic source imaging, and intracranial stereo-electroencephalography in focal cortical dysplasia. *Neuroimage-Clinical*, 2017, 15, pp.71 - 79. 10.1016/j.nicl.2017.04.018 . hal-03962921

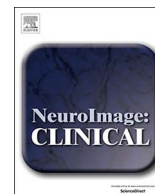
HAL Id: hal-03962921

<https://hal.science/hal-03962921>

Submitted on 30 Jan 2023

HAL is a multi-disciplinary open access archive for the deposit and dissemination of scientific research documents, whether they are published or not. The documents may come from teaching and research institutions in France or abroad, or from public or private research centers.

L'archive ouverte pluridisciplinaire **HAL**, est destinée au dépôt et à la diffusion de documents scientifiques de niveau recherche, publiés ou non, émanant des établissements d'enseignement et de recherche français ou étrangers, des laboratoires publics ou privés.



The relationship between morphological lesion, magnetic source imaging, and intracranial stereo-electroencephalography in focal cortical dysplasia



Romain Bouet^{a,b}, François Mauguière^{b,c,e}, Sébastien Daligault^{a,b,d}, Jean Isnard^{b,c,e},
Marc Guenet^{b,c,e}, Olivier Bertrand^{a,b}, Julien Jung^{a,b,c,*}

^a Lyon Neuroscience Research Center, INSERM U1028, CNRS UMR5292, Brain Dynamics and Cognition Team, Lyon F-69000, France

^b Université Lyon 1, Lyon F-69000, France

^c Hospices Civils de Lyon, Neurological Hospital, Functional Neurology and Epileptology Dept, Lyon F-69003, France

^d CERMEP - Imagerie du vivant, Bron F-69003, France

^e Lyon Neuroscience Research Center, INSERM U1028, CNRS UMR5292, Central Integration of Pain, Lyon F-69000, France

ARTICLE INFO

Keywords:

Partial seizures
Focal cortical dysplasia
Intracranial EEG
Epileptogenic zone
MEG

ABSTRACT

Magnetoencephalography (MEG) is a useful non-invasive technique for presurgical evaluation of focal cortical dysplasia patients. We aimed at clarifying the precise spatial relationship between the spiking volume determined with MEG, the seizure onset zone and the lesional volume in patients with focal cortical dysplasia.

We studied the spatial relationships between the MEG spiking volume determined with a recent analysis pipeline, the seizure-onset zone location determined with a quantitative index calculated from intracranial EEG signals ('Epileptogenicity Index') and the lesional volume delineated on brain MRI in 11 patients with Focal Cortical Dysplasia explored with Stereo-electroencephalography (SEEG).

A significant correlation between the MEG spiking activity and the Epileptogenicity Index was found in 8/11 patients. 7/8 patients were operated upon and had good surgical outcome. For three patients, no correlation between Epileptogenicity Index and spiking activity was observed; only one of those three patients had good surgical outcome.

The lesion was at least partially overlapping with the seizure-onset zone in 8/9 patients with a lesion clearly identifiable by MRI. However, 57% of the SEEG epileptogenic contacts were located outside of the lesional volume. Lastly 44% of the highly epileptogenic SEEG contacts were located within the spiking volume and 22% of them were located exclusively in the spiking volume and not in the lesion. For 7/9 patients with a lesion, < 50% of epileptogenic SEEG contacts were included within the lesion: for 5/7 patients MEG provided an added value for targeting the epileptogenic region through intracranial electrodes, while for two of seven patients MEG detected only a few extralesional epileptogenic contacts.

Our study suggests that modeling of the spiking volume with MEG is a promising tool to localize non-invasively the seizure-onset zone in patients with focal cortical dysplasia. Combined with brain MRI, MEG modeling of the spiking volume contributes to delineate the spatial extent of the seizure-onset zone.

1. Introduction

Focal cortical dysplasia (FCD) results from abnormal neuronal migration and is a very common cause of pharmaco-resistant epilepsy. Surgical treatment often requires intracranial electroencephalography recordings to localize the seizure onset zone (SOZ) and seizure propagation pathways (Fauser et al., 2015; Guerrini et al., 2015; Ryvlin et al., 2014). Moreover, the surgical outcome in FCD related epilepsy is directly related to the resection of epileptogenic tissue

(Fauser et al., 2015, 2008; Hong et al., 2000).

While numerous studies have shown that FCD is intrinsically epileptogenic, recent intracranial EEG studies have challenged the idea that epilepsy in FCD is associated with a strictly focal epileptogenic zone. Seizure can be triggered by discrete hyper-excitabile cortical patches but also by additional remote epileptogenic areas of cortex, which may appear normal on brain MRI (Aubert et al., 2009; Chassoux et al., 2000; Tassi et al., 2001; Widdess-Walsh et al., 2007). Moreover, despite undisputed methodological advances of MRI acquisition and

* Corresponding author at: Lyon Neuroscience Research Center, CRNL, INSERM, U1028 – CNRS, UMR5292, Brain Dynamics and Cognition Team, Centre Hospitalier Le Vinatier (Bâtiment 452) 95, Boulevard Pinel, Lyon, 69500 Bron, France.

E-mail address: julien.jung@chu-lyon.fr (J. Jung).

<http://dx.doi.org/10.1016/j.nicl.2017.04.018>

Received 5 January 2017; Received in revised form 14 April 2017; Accepted 18 April 2017

Available online 20 April 2017

2213-1582/ © 2017 The Authors. Published by Elsevier Inc. This is an open access article under the CC BY-NC-ND license (<http://creativecommons.org/licenses/by-nc-nd/4.0/>).

MRI post-processing, the precise evaluation of the spatial extent of the lesion still remains a challenging issue (Battal et al., 2015; Bernasconi et al., 2011; Colombo et al., 2012). There is therefore a need for a better detection and evaluation of the involvement of these distributed epileptogenic foci that should improve surgical efficacy in patients with FCD.

Interictal epileptiform discharges have been suggested as a surrogate marker of epileptogenic areas and are usually abundant within the FCD lesion. Interictal spikes recorded with MEG and EEG can reliably be modeled with source modeling procedures (Bouet et al., 2012; Jung et al., 2013; Agirre-Arrizubieta et al., 2009; Englot et al., 2015; Knowlton et al., 2006). It has been shown that the sources of interictal spikes recorded with MEG or EEG in FCD are usually in close vicinity of the MRI lesion and of the SOZ (Bast et al., 2004; Wang et al., 2014; Widjaja et al., 2008; Wilenius et al., 2013). However, in most studies, the spikes are modeled with single dipole models, which cannot directly estimate the true extent of the irritative zone, and the spatial extent of the SOZ is based on visual analysis of seizures on intracranial EEG recordings of seizures, but not on quantitative markers of the ictal discharges. Hence, the spatial overlap between the irritative zone, the lesion and the SOZ is only indirectly evaluated in these studies (Bast et al., 2004; Wang et al., 2014; Widjaja et al., 2008; Wilenius et al., 2013).

In the present study, we sought to evaluate precisely the spatial relationship of the irritative zone, the MRI lesion and the SOZ using quantitative electrophysiological markers in FCD patients. We used a method that estimates the volumetric sources of interictal spikes (Volumetric Imaging of Epileptic Spikes or VIES, Bouet et al., 2012) recorded by MEG for delineating the irritative zone, and a quantitative index based on both spectral and temporal properties of intra-cerebral ictal EEG signals for assessing the SOZ spatial extent (Bartolomei et al., 2008).

We hypothesized that magnetic source imaging (MSI) based on VIES could provide information regarding the spatial distribution of the SOZ, and might show epileptogenic areas both in the lesion area but also in regions located in the vicinity or remotely from the brain lesion.

2. Materials and methods

2.1. Patients

We retrospectively included all patients with focal epilepsy related to FCD who had undergone presurgical evaluation in the Epilepsy Department of the Neurological Hospital, Lyon, France between 2006 and 2012 and who fulfilled the following inclusion criteria: a) intracranial EEG recordings with stereotactically implanted electrodes (SEEG) (Bancaud et al., 1969); b) MSI of epileptic spikes with VIES (Bouet et al., 2012); c) either histo-pathological diagnosis of FCD for patients operated upon or brain MRI highly suggestive of FCD in patients discarded from surgery.

In the classification of FCDs we used the consensus classification proposed by the ILAE 2011 (Blumcke et al., 2011). Brain MRI was considered as very suggestive of FCD if one or several of the following established characteristic MRI features were detected by visual inspection by an expert neuroradiologist and validated by the epilepsy multidisciplinary group that includes the epileptologists and neurosurgeons of our department (Battal et al., 2015; Colombo et al., 2012). These features include: i) focal cortical thickening; ii) blurring of the grey–white matter interface; iii) focally increased signal on T2-weighted Imaging or FLAIR sequences (cortical or subcortical) and; iv) a tail of increased signal from the cortex to an underlying ventricle on T2- or FLAIR sequences. Patients were considered MRI-negative if MRI disclosed no abnormalities, or only subtle abnormalities of unclear significance.

Six male and five female patients with a mean age of 22.4 years (range 9–41) were included (Table 1). Ten patients were operated upon

Table 1
Overview of the clinical features of the 11 patients with MRI lesion, MEG spiking volume localization and surgical treatment.

Patient	Age	Gender	Epilepsy duration	Seizure frequency	MRI lesion location	Lesional volume (mm ³)	MEG spiking volume (mm ³)	MEG localization	SEEG SOZ	Surgery	Pathology	Surgical outcome	Overlap MEG SV/resection
Pt1	18	F	6	1/wk	Left OFC	4747	47,289	Left OFC	Left OFC	Left OFC	FCD IIa	Ia (6 m)	Y
Pt2	41	M	23	2/m	No lesion	0	17,923	Right Ant-T	Right Ant-T	Right Ant-T	FCD I	Ib (48 m)	Y
Pt3	24	F	7	2–3/wk	Left Lat-O/no lesion in T lobe	3652	31,901	Left Ant-T	Left Ant-T	Left Ant-T	HS	Ia (48 m)	Y
Pt4	33	M	10	1/m	Left C	8808	40,200	Left C	Left C + left DLF	NA	NA	NA	NA
Pt5	20	M	10	1/wk	Right C	7354	43,172	Right C	Right C	Right C	FCD I	Ia (6 m)	Y
Pt6	30	F	8	3–4/wk	Left Lat-P	5901	22,217	Left Lat-P	Left Lat-P	Left Lat-P	FCD IIa	II (48 m)	Y
Pt7	15	M	8	2/wk	Right Mes-O	31,217	46,237	Right Lat-O	Right Lat-O	Right Lat-O	FCD III	II (24 m)	Y
Pt8	9	M	5	3/m	Right Ant-T	16,892	19,340	Right Ant-T	Right Ant-T	Right Ant-T	FCD IIa	Ia (24 m)	Y
Pt9	26	F	16	1/m	Right DLF	22,723	20,416	Right C	Right DLF	Right DLF	FCD IIa	III (36 m)	N
Pt10	21	M	10	1/wk	No lesion	0	12,510	Left post-P	Left C + left P	Left C + left P	FCD IIa	Ia (24 m)	Y
Pt11	10	F	7	4/wk	Left C/left Lat-P	47,933	85,003	Left DLF	Left C + left DLF	Left F + left C disconnection	FCD IIa	III (15 m)	Y

Age: age at SEEG in years – epilepsy duration: epilepsy duration in years – seizure frequency: wk = week; m = month – MRI lesion: the anatomical localization of the MRI lesion is provided (no lesion: absence of MRI detectable lesion/DLF; Dorso Lateral Frontal/OFC; Orbito Frontal/T: Temporal/O: Occipital/P: Parietal/C: Central/Lat: Lateral/Mes: Mesial/Ant: Anterior/Post: Posterior) – Lesional Volume: volume of the MRI lesion in mm³ after manual delineation on co-registered MRI sequences – MEG spiking volume: The extent of the MEG spiking volume in mm³ was determined by VIES (see material and methods) – MEG localization: Localization of the voxel with maximal spike related activity determined with VIES (same legend as MRI lesion) – SEEG SOZ: Localization of the SOZ determined with SEEG (same legend as MRI lesion) – Surgery: site of resection (same legend as MRI lesion) – Pathology: FCD: Focal Cortical Dysplasia/HS: Hippocampal Sclerosis/NA: not applicable – Overlap MEG SV/resection: Y: yes/N: no/NA: not applicable — Surgical Outcome: outcome is expressed as Engel Score (length in follow-up in months is provided)/NA: not applicable.

while one patient was discarded from surgery (for that patient, the seizure onset zone was overlapping with the primary motor cortex). Of the ten operated patients, eight had a favorable outcome following surgery (Engel Class I or II) (Engel and Rasmussen, 1993) and two had a poor outcome (Engel Class III or IV) after a median follow-up of 23.1 months (range 6–48).

2.2. Depth stereotactic EEG recordings (video-SEEG)

Ictal and interictal intracranial video-SEEG recordings were obtained in all 11 patients.

SEEG explorations were carried out during long-term video-EEG monitoring. Recordings were performed using intracerebral electrodes with multiple contacts (Dixi Medical (France), 10–15 contacts, length: 2 mm, electrode diameter: 0.8 mm, intercontact spacing 1.5 mm) placed according to Talairach's stereotactic method. The number of electrodes implanted per patient varied between 7 and 18, with a total number of recording contacts between 90 and 114 per patient. Electrodes were left in place between one and three weeks. When MRI disclosed a lesion with typical features of FCD, it was always targeted by one or a few depth electrodes ($n = 9/9$ patients).

2.3. MRI acquisition

In all patients, brain MRI was performed using a 3 T MR scanner (Philips Achieva, Philips, Best, The Netherlands), and included the following sequences in all patients: (i) 3D anatomical T1-weighted covering the whole brain volume with 1 mm^3 cubic voxels; (ii) six-millimeter-thick turbo-spin echo T2-weighted acquired in the bi-hippocampal plane; (iii) three-millimeter-thick turbo-spin echo T2 perpendicular to the bi-hippocampal plane; (iv) three-millimeter-thick inversion-recovery; (v) 3D FLAIR volumetric images with isotropic resolution of 1 mm^3 voxels.

In the 24 h following electrode implantation, a second MRI 3D T1 sequence was obtained to show the exact location of recording contacts.

2.4. MEG acquisition

MEG signals were recorded on a CTF Omega 275 channel whole head system (VSM MedTech Ltd., Canada). For each patient, 45 min of continuous MEG signal were recorded at a sampling frequency of 600 Hz using a third-order spatial gradient noise. Patients were investigated at rest with their eyes closed. Three fiducial coils (nasion, left and right pre-auricular points) were placed for each patient to determine the head position within the MEG helmet, and to provide co-registration with the anatomical MR images.

2.5. MEG modeling of the sources of interictal spikes

MEG data were processed using VIES, a pipeline of analysis previously described and validated. VIES aims at localizing the brain spiking volume (SV) which generates high frequency activities (> 20 Hz) associated with interictal spikes (see Bouet et al. (2012) for a full description of the method).

In VIES, spikes are first visually identified on raw MEG signals. Secondly, the brain sources of spike-related high frequency activity (> 20 Hz) are located using a beamforming technique, DICS (Dynamic Imaging of Coherent Sources) (Gross et al., 2001), comparing the source power for high-frequency during the spike period and a baseline period. The brain sources of spike-related high frequency activity were computed for all 5 mm^3 voxels covering the brain volume, providing whole-brain MEG maps. Lastly, the whole-brain MEG maps are thresholded using a method described in Bouet et al. (2012), providing a MEG spiking volume map (MEG SV) for each patient (see Fig. 1-D).

2.6. Definition of the seizure-onset zone using SEEG signals

For each patient, we extracted all SEEG signals recorded during spontaneous seizures. In order to estimate the SOZ, we used a quantitative index (Epileptogenicity Index EI) based on a method previously described by Bartolomei et al. (2008). In the present study, EI is a quantity computed for each pair of bipolar EEG contacts that accounts for the propensity of a brain area to generate rapid discharges (above 12 Hz) during the 10 s following seizure-onset. For each contact, EI is normalized by dividing its EI actual value by the maximal value obtained in each patient. Please see Supplementary Material for a full description of EI computation.

2.7. Estimating the spatial relationship between the seizure-onset zone and the MEG spiking volume (SV)

For each patient, we co-registered the location of all SEEG electrodes and whole-brain MEG maps and we determined the individual MEG voxel associated with each SEEG pair of neighboring contacts. Then we extracted the source power of high-frequency spike related activity corresponding to these voxels and their corresponding EI value. Lastly, a simple linear correlation between the MEG source power and the EI values was searched. A p -value of 0.05 was considered to be statistically significant. This analysis was firstly performed in each individual and secondly by pooling the data of all patients.

We also tested the spatial congruence between the MEG voxel disclosing maximal high-frequency spike related activity and the intracranial EEG contact with maximal EI value using predefined anatomical subregions (temporal pole, mesial temporal region, anterior temporal neocortex, posterior temporal neocortex, temporo-basal region, dorso-lateral frontal cortex, mesial frontal cortex, orbito-frontal cortex, central region, lateral parietal cortex, mesial parietal cortex, lateral occipital cortex, mesial parietal cortex, insula). We considered that both were congruent if they were located in the same anatomical sub-region.

2.8. Estimating the spatial congruence between the MRI lesion, the seizure-onset zone and the MEG spiking volume (SV)

In a first step, for patients with a clear FCD lesion on brain MRI, we co-registered 3D-T1 and FLAIR sequences in different planes (axial, sagittal and coronal). The brain lesion of each patient was manually delineated (Fig. 1-C) using the free software Anatomist (Rivière et al., 2011). We considered not only cortical abnormalities (abnormal gyration, signal abnormalities) but also abnormal blurring of the grey and white matter junction and abnormal signal of the white matter for the delineation. In a second step, the MEG maps of source power of high-frequency spike related activity were thresholded according to the Bouet et al. (2012) procedure. This procedure provided a MEG spiking volume (MEG SV) for each patient (Fig. 1-D). In a last step, we defined the SOZ on SEEG signals using EI values, considering that high EI values (above 0.3) indicated highly epileptogenic regions. Please note that this cut-off score was determined by plotting all computed EI values across patients, showing that the 0.3 value corresponded to the 90th percentile of all EI values.

In a first global analysis, we tested whether there was a spatial congruence between the brain lesion and the MEG SV. We considered that both volumes were congruent if the lesion and the MEG SV were at least partially overlapping.

In a second analysis, we counted the proportion of highly epileptogenic contacts within the lesion volume, within the MEG SV, and within the union of both. We also counted the proportion of highly epileptogenic contacts that were included solely either in the MEG SV, or in the lesion volume, or in the intersection of MEG SV and lesion volume.

The second analysis was performed for each patient and at the group level.

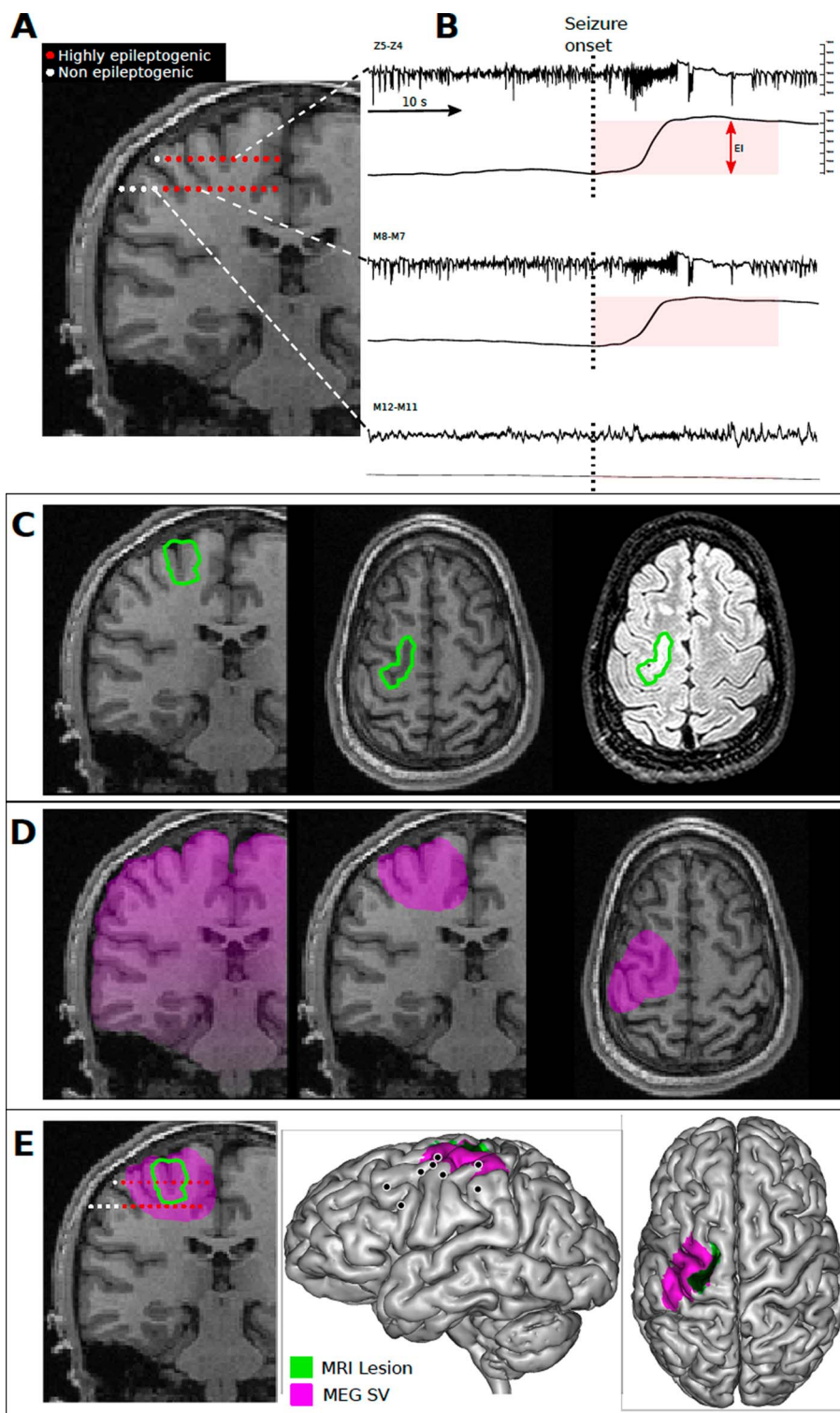


Fig. 1. Overview of the method evaluating the spatial overlap between the MEG spiking volume, the Seizure-Onset Zone determined with SEEG and the MRI lesion in patients with Focal Cortical Dysplasia. **A**) Example of depth electrode implantation for stereoelectroencephalographic (SEEG) exploration in a patient with focal cortical dysplasia (Pt5). The electrode trajectories are superimposed on the coronal MRI. Electrode contacts in red are included in the SOZ and electrode contacts in white are not included in the SOZ. **B**) The epileptogenicity (Epileptogenicity Index EI) of each pair of bipolar contacts is derived from a slightly modified method initially described by Bartolomei et al. This method estimates the EI that accounts for the propensity of a brain area to generate rapid discharges (above 12 Hz) during the 10 s following seizure-onset. On the right panel, raw SEEG traces (SEEG) are shown for three electrode contacts (Z5-Z4, M8-M7 and M12-M11), and their corresponding high frequency activity at seizure onset is shown (CuSum Value). The EI is the height of the CuSum Value at seizure onset (Cumulative Sum of high frequency activity during the 10 s following seizure-onset time, shown as a pink period). Please note that Z5-Z4 is more epileptogenic than M8-M9 and that no significant seizure activity is observed for M12-M11. **C**) The focal cortical dysplasia was manually delineated on T1 and FLAIR sequences (green area). **D**) The high frequency activity (above 20 Hz) associated with MEG spikes was determined for all voxels within the brain and the maps were thresholded according to the Bouet et al. (2012) procedure to obtain the MEG spiking volume (purple area). **E**) The spatial relationship between the SOZ, the SV and the brain lesion was evaluated by co-registering electrode contacts displaying elevated EI, the MEG SV, and the brain lesion. Please note that for Pt5, most highly epileptogenic contacts (red contacts) were located both within the brain lesion and the MEG SV, but some highly epileptogenic contacts were specific to the MEG SV (not within the lesion). A lateral view of all depth electrodes superimposed on a 3D reconstruction of the neocortical surface of the brain superimposed on a 3D reconstruction of the neocortical surface of the brain is represented on the right side, with a projection of MEG SV shown in purple and of the brain lesion in green.

Table 2

Overlap between the seizure-onset zone, the MEG spiking volume (SV) and the MRI lesion in all 11 patients with FCD.

Patient	N SEEG contacts	Correlation between MEG Spiking Activity and SEEG EI	Volume overlap		Spatial congruence between epileptogenic zone/lesion/MEG SV				
			MEG SV within lesion (%)	Lesion within MEG SV (%)	Epileptogenic contacts within MEG SV (%)	Epileptogenic contacts within lesion (%)	Epileptogenic contacts within intersection of lesion & SV (%)	Epileptogenic contacts specific to MEG SV (%)	Epileptogenic contacts specific to lesion (%)
Pt1	106	Y	3	83	86	100	86	0	14
Pt2	112	Y	0	0	0	0	0	0	0
Pt3	113	Y	0	0	100	0	0	100	0
Pt4	114	Y	18	80	60	56	48	12	8
Pt5	90	Y	13	77	80	25	23	57	2
Pt6	91	Y	4	13	33	33	0	33	33
Pt7	102	Y	4	6	19	35	12	8	23
Pt8	101	Y	37	43	50	50	50	0	0
Pt9	92	N	3	2	17	100	17	0	83
Pt10	110	N	0	0	33	0	0	33	0
Pt11	105	N	12	22	0	70	0	0	70
Mean			8	30	44	43	21	22	21

2.8.1. Standard protocol approvals, registrations, and patient consents

The study was approved by the local ethics committee, and written consent was obtained.

3. Results

3.1. Estimating the spatial relationship between the seizure-onset zone and the MEG spiking volume (SV)

For the whole group of patients, after pooling all data across patients, a significant linear correlation was observed between spike-related high frequency activity derived via MEG and EI values via SEEG ($p < 0.01$, Pearson correlation).

At the individual level, we found for 8/11 patients a significant linear correlation between spike-related high frequency activity and EI values ($p < 0.01$, Pearson correlation, see Table 2). Moreover, for these eight patients, we found that the voxel with maximal spike-related high frequency activity was always located within the same sublobar region lobe as the intracranial contacts with maximal EI value (Table 1).

For three patients, the correlation coefficients were not significant. For these three patients, the MEG voxel with maximal spike-related high frequency activity was located in the same lobe as the intracranial contacts with maximal EI value, but not in the same sublobar region.

3.2. Estimating the spatial congruence between the MRI lesion, the seizure-onset zone and the MEG spiking volume (SV)

The MEG SV at least partially overlapped with the lesion in all patients but one (Table 2). However, only a small portion of the MEG SV overlapped with the lesion volume (between 3 and 37%, mean 8%). For most patients, a higher proportion of the lesion volume was included in the MEG SV (between 2 and 83% of the lesion was included within the MEG SV, mean 30%).

In a second analysis, we determined the proportion of highly epileptogenic contacts within the lesion volume, within the MEG SV, and within the intersection of MEG SV and lesion volume (Table 2). We found that the proportion of highly epileptogenic contacts included in the MEG SV was variable across patients and (mean 44% range 0–100), and that the proportion of highly epileptogenic contacts included within the lesion was roughly identical and also highly variable (mean 43% range 0–100). For four patients, the number of epileptogenic contacts included in the MEG SV was higher than that included in the lesion, while it was the reverse in four patients. For one patient, both numbers were equal. At the intersection of MEG SV and lesion, the proportion of epileptogenic contacts detected was 21% (range 0–86%).

This suggests that the sensitivity of the MEG SV and that of the lesion volume for the detection of epileptogenic contacts are roughly identical at the group level, but more heterogeneous at the individual level. At the group level, 65% of the epileptogenic contacts were included in the brain area encompassing both the lesion and the MEG SV.

Lastly, we determined the proportion of highly epileptogenic contacts that were included solely in the lesion volume, solely in the MEG SV or solely in the intersection of MEG SV and the lesion volume (Table 2). We found that the mean proportion of highly epileptogenic contacts that were specific to the MEG SV was 22% (range 0–100%), and that the proportion of highly epileptogenic contacts that were specific to the lesion was 21% (range 0–83%). For four patients, more epileptogenic contacts were specific to the MEG SV, while for four patients more epileptogenic contacts were included in the lesion than in the MEG SV. For seven patients, < 50% of epileptogenic contacts were included in the lesion: for five of those seven patients, at least 20% of the epileptogenic contacts were detected exclusively by MEG.

To illustrate the relative sensitivity of MEG and brain lesion to detect epileptogenic regions in FCD, two figures representing different clinical situations are shown. Fig. 2 illustrates a patient for whom the brain lesion and the MEG SV provide complementary information regarding the epileptogenic cortex. Fig. 3 illustrates a patient for whom the lesion is distant from epileptogenic contacts and the MEG SV. Please also see Supplementary Fig. 1 which illustrates the lesion volume (MRI), the spiking volume (MEG), and contacts with high EI (SEEG) for all patients with a lesion on brain MRI.

Lastly, Fig. 4 summarizes the main results concerning the spatial congruence between the MRI lesion, the Seizure-Onset Zone and the MEG spiking volume (SV).

In 9/10 patients operated upon, the resected area (determined by surgical report and post-operative CT-scan) overlapped with the MEG SV and the MEG voxel having maximal high-frequency spike related activity was included in the resected area. For two of those nine patients, brain MRI was negative. 6/10 patients were classified Engel I post-operatively, 2/10 patients were classified Engel II post-operatively and 1/10 patient was Engel III.

For a single patient (Pt9), the MEG SV was slightly posterior to the surgical resection. Pt 9 was classified Engel III post-operatively.

For 7/8 patients with a clear MRI lesion operated upon, the resection area overlapped with the lesion. For 1/8 patient (Pt3), the surgical resection targeted a brain region located remotely from the lesion.

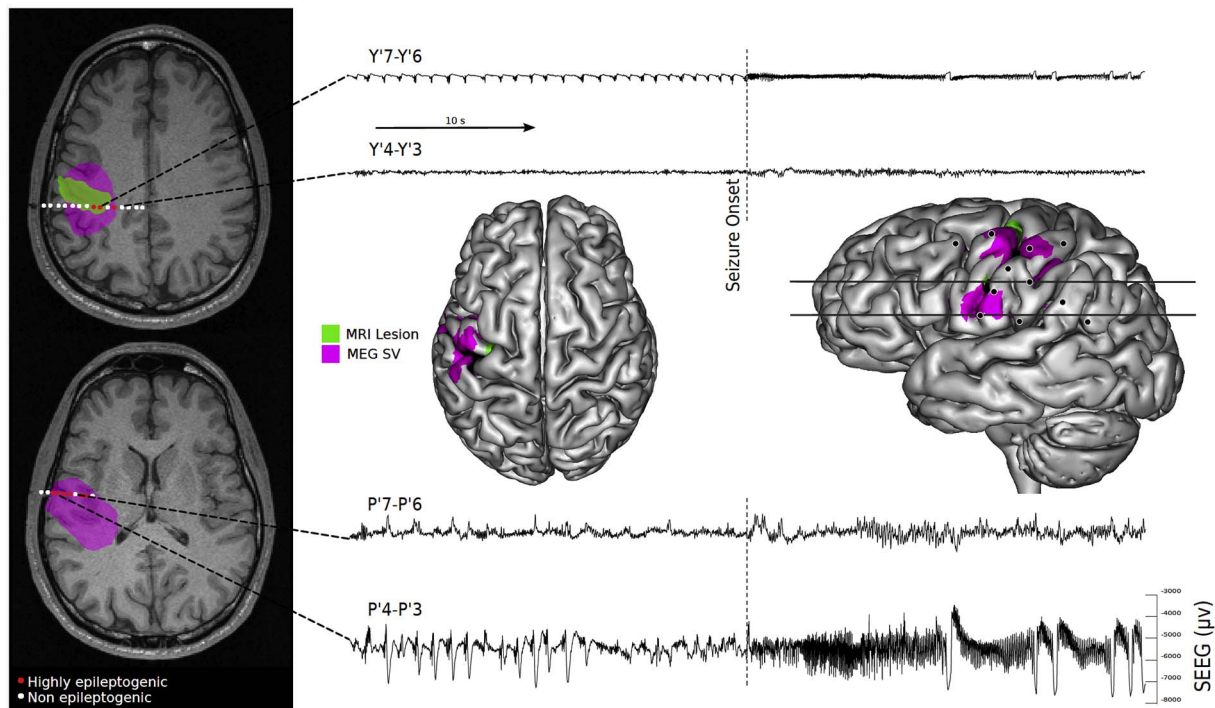


Fig. 2. Example of a patient (Pt4) with FCD for whom the brain lesion and the MEG SV provide complementary information regarding the epileptogenic cortex. The trajectories of the SEEG electrodes are superimposed on the axial MRI. Highly epileptogenic contacts are in red and non-epileptogenic contacts are in white. The green area represents the lesional area manually delineated on brain MRI. The purple area represents the MEG SV. The lesional area and MEG SV are also projected on a 3D reconstruction of the neocortical surface of the brain and some examples of raw SEEG traces are also shown. Please note that the MEG SV, the brain lesion and the SOZ were largely overlapping in this case. However, the MEG SV was more spatially extensive than the SOZ, and some highly epileptogenic contacts were specific to the MEG SV.

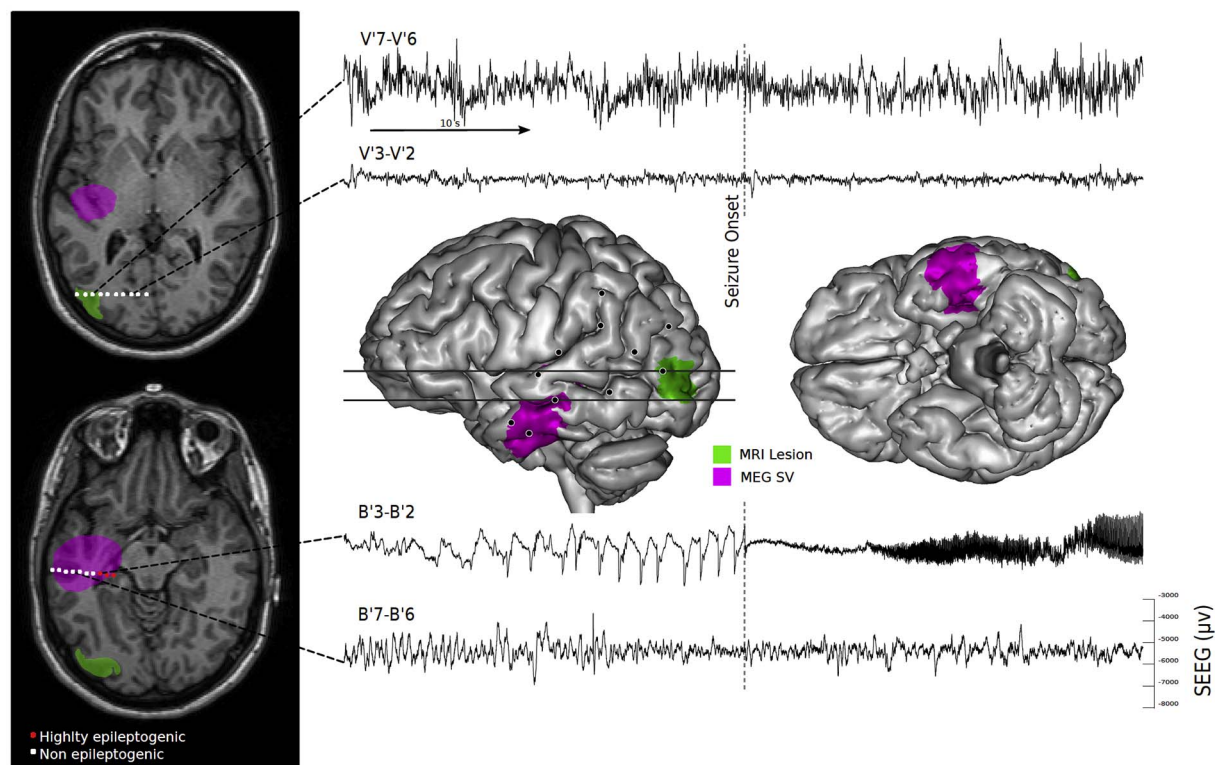


Fig. 3. Example of a patient (Pt3) with FCD for whom the SOZ was located remotely from the MRI lesion and was overlapping with the MEG spiking volume. The trajectories of the SEEG electrodes are superimposed on the axial MRI. Highly epileptogenic contacts are in red and non-epileptogenic contacts are in white. The green area represents the lesional area manually delineated on brain MRI. The purple area represents the MEG SV. The lesional area and the MEG SV are also projected on a 3D reconstruction of the neocortical surface of the brain and some examples of raw SEEG traces are shown. Please note that there was clearly no spatial overlap between the lesion, which had typical MRI features of FCD and the SOZ (the lesion was in the occipital lobe and the SOZ in the temporal lobe). However, highly epileptogenic contacts were detected by MEG.

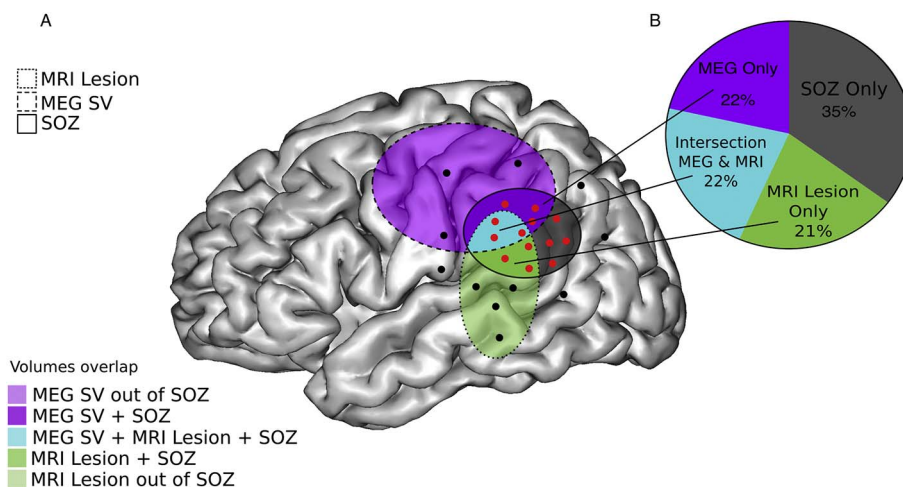


Fig. 4. Spatial overlap between the MRI lesion, the MEG spiking volume and the Seizure-Onset Zone in 9 FCD patients. A) Schematic view of the brain and volume overlap. Dark purple area: spatial overlap between MEG SV and the SOZ/Light purple area: spatial overlap between MEG SV, lesional volume and the SOZ/Light green area: Lesional volume not involved in seizure activity/Dark green area: spatial overlap between lesional volume and the SOZ/Blue area: spatial overlap between the MEG SV, lesional volume and the SOZ/Gray area: portion of the SOZ outside of the MEG SV and lesional volume. SEEG electrodes showing clear signal change at seizure onset (and with high EI values) are shown in red and electrodes without ictal changes (with low EI values) are shown in black. The SOZ is defined by the region encompassing all SEEG electrodes in red. B) Schematic view of spatial overlap between the SOZ, the lesional area and the MEG SV. The proportion of the all epileptogenic contacts included in the MEG SV only (MEG only), in the lesional area only (lesion only), in the intersection of the MEG SV and lesional areas (intersection) and outside of the MEG SV and lesional area across the nine patients is displayed in the pie chart.

4. Discussion

4.1. Epileptogenicity of FCD

Focal cortical dysplasias (FCDs) are a common cause of pharmacoresistant epilepsy, prompting presurgical evaluation in a large proportion of patients (Guerrini et al., 2015). Their localization, extent, and histo-pathologic presentation are highly variable, reflected in several consensus classification schemes.

Several reports have shown that FCD are intrinsically epileptogenic (Hong et al., 2000; Ferrer et al., 1992; Morioka et al., 1999; Otsubo et al., 2005; Palmini et al., 1995). Thus, intracranial EEG studies show intralesional rhythmic spike discharges in the interictal periods, spontaneous ictal discharge onset and a low threshold of seizure induction after electrical stimulation in the lesion (Aubert et al., 2009; Chassoux et al., 2000; Tassi et al., 2001; Avoli et al., 1999; Matsumoto et al., 2005; Varotto et al., 2012). Moreover, the completeness of lesional resection is an important determinant of surgical outcome (Fauser et al., 2015, 2008; Hong et al., 2000; Francione et al., 2003; Lee and Kim, 2013).

In accordance with those findings, we found that for 8/9 patients with a typical FCD on brain MRI, the lesion was overlapping the SOZ (defined by quantitative EEG analysis). More precisely, we observed that 42% of the highly epileptogenic contacts were located directly within the lesion, suggesting that a large proportion of the SOZ was included within the lesion. Lastly, for 7/8 patients operated upon, the surgical resection included the lesional area.

We found that the MEG SV was also tightly related to the MRI lesion and the SOZ. Indeed, for 8/9 patients with a clear MRI lesion, the MEG SV was overlapping with the lesion, even if the MEG SV was more widespread than the lesion. Moreover, for 8/11 patients, there was a significant correlation between intracranial epileptogenicity and MEG spiking activity. For those 8 patients, the MEG source with maximal spike-related activity was located within the same sublobar region lobe as the seizure-onset zone. As a whole, 44% of the highly epileptogenic contacts were included in the MEG SV.

Taken together, these results show that for most of the patients, the MRI lesion, the MEG SV and the SOZ are co-extensive brain areas. This result is in accordance with several earlier studies, using EEG or MEG with different source modeling approaches showing that the sources of epileptic spikes are co-extensive with the MRI lesion (Wilenius et al.,

2013; Bast et al., 2006; Itabashi et al., 2014). However, in most of these studies, it is hard to extract a quantitative value of the spatial overlap between the MEG spiking volume and the MRI lesion, since classical equivalent current dipole models do not provide a direct estimation of the spiking volume. Several studies have also shown that the sources of epileptic spikes are also in close vicinity with the seizure generating area, both for patients with visible MRI lesion and for the more challenging group of negative-MRI patients (Wang et al., 2014; Widjaja et al., 2008; Wilenius et al., 2013; Ishibashi et al., 2002; Ishii et al., 2008). However, in those studies, the epileptogenicity of the dysplastic cortex and of surrounding intracranial EEG contacts is not directly quantified and it is thus difficult to estimate precisely the relationships between the lesion, surrounding cortex and the SOZ.

4.2. Epileptic networks in FCD

Several arguments show that MRI is not sufficient to plan surgical resection and that the epileptogenic zone can be more extended than the visible lesion on MRI.

Firstly, despite optimal MRI acquisition sequences, careful examination of MRI slices and advanced post-processing of the images, FCD remains occult on MRI images for some patients with pathologic confirmation of the dysplasia (Battal et al., 2015; Bernasconi et al., 2011). In the present study, two of our 11 patients were clearly MRI negative. In these 2 patients, MEG was very helpful to guide the SEEG electrode implantation.

Secondly, for some patients, the SOZ can be located remotely from the MRI lesion itself as.

in one of our patients (Pt3) for whom there was clearly no spatial overlap between the lesion, which had typical MRI features of FCD, and the SOZ (the lesion was in the occipital lobe and the SOZ in the temporal lobe) (Fig. 3). For this patient, SEEG implantation strategy was mostly guided by clinical symptoms and MEG which suggested temporal lobe involvement. That observation highlights the fact that in rare cases the MRI lesion can misguide the localization of the true SOZ in FCD.

Lastly, while the lesion is usually considered as the core of the seizure-generating region in FCD patients, a still controversial question is to what extent seizures originate within the dysplastic cortex, in the surrounding brain or in both regions (Guerrini et al., 2015).

In our study, we found that approximately half of the highly

epileptogenic contacts were not directly located within the MRI lesion, but in the surrounding cortical areas. This result clearly shows that the spatial extent of the SOZ cannot be fully delimited by the MRI lesion.

Even in patients with a clear MRI lesion, other neuroimaging tools such as MEG may thus bring complementary information to estimate the extent of the SOZ. Indeed, for seven patients, < 50% of epileptogenic contacts were included in the lesion: for five of those seven patients, MEG provided additional information regarding epileptogenic contacts (at least 20% of the epileptogenic contacts were detected exclusively by MEG in these five patients).

This suggests that the spiking volume estimated with MSI can bring additional information regarding the spatial extent of the SOZ when epileptogenic areas outside from the lesion area.

Our results are in accordance with several studies showing that FCD may be associated with multiple areas of epileptogenicity, some of which are structurally normal. For instance, Aubert et al. (2009) using the original computation of the Epileptogenicity Index in 36 patients with MCDs investigated by SEEG found that 30% of patients had a strictly focal epileptogenic zone organization while the remaining patients had more than one epileptogenic region, disclosing a network or bilateral epileptogenic zone organization (Aubert et al., 2009). In a study by Chassoux et al. (2000), using the same SEEG approach as in this study, 20% of patients with FCD were considered to have an epileptogenic zone larger than the dysplastic cortex (Chassoux et al., 2000).

As a whole, our study and those earlier studies suggest that epileptic networks in Focal Cortical Dysplasia can be more widespread than the MRI lesion.

From a theoretical perspective, the surgical resection of FCD patients should include all seizure-generating areas, not only those located in close vicinity of the lesion, but also remote epileptogenic regions. Our results strongly suggest that the results of MEG spike modeling should be used to determine the sites of SEEG electrode implantation. However, whether MEG SV determination should be used to optimize surgical resection in FCD patients is still an open question. At the time of the study, MEG data were not used to determine the to-be-resected areas in our patients. Further studies are necessary to correlate the surgical prognosis and the extent of resection of the irritative zone determined by MEG.

4.3. Limitations of the study

The main limitation of this work is related to the incomplete and inhomogeneous brain exploration provided by SEEG. SEEG recordings enable a fine-grained analysis of neural activity for selected brain regions but a large portion of the brain is not covered by SEEG electrodes. This suggests that it is not possible to exclude that some epileptogenic areas were not detected. On the contrary, MEG source analysis provides a homogeneous and exhaustive view of the cerebral cortex, but with lower spatial resolution. Those intrinsic limitations of SEEG may partly explain why for a few patients, no correlation between SEEG EI and MEG spiking activity was found (Pt 9, 10 and 11). Indeed, for two of those patients, the surgical outcome was poor, suggesting that the true SOZ was not detected. Another explanation could be related to the limited spatial resolution of MEG. We recently shown that the spatial accuracy of the VIES method for the determination of the spiking volume is high and clinically meaningful (Bouet et al., 2012). However, the specificity of the method is imperfect, so that the spiking volume determined with VIES is usually more widespread than the spiking volume determined with intracranial EEG. Those limitations may explain while the maximal spiking activity for those three patients was in the same lobe as the SOZ but not in the same sublobar region.

Another limitation of the study is related to the fact that we deliberately focussed on MEG and MRI contribution for surgical strategy of FCD patients. The strategy of SEEG electrode implantation in our centre relies on several investigations, including detailed

semiological analysis of seizures recorded during video-EEG telemetry, careful brain MRI reviewing by several experts, FDG PET and MEG. A multimodal approach is therefore used to evaluate the strongest hypothesis regarding SOZ location and to guide SEEG electrode placement. In FCD patients with frequent spikes, MEG is a powerful technique to localize the SOZ and is particularly helpful when MRI is negative (such as Pt 2 and 10) or discloses an ambiguous lesion (such as Pt3). However, further study is needed to clarify the respective roles of FDG PET, MEG, MRI for optimal targeting of the SOZ with SEEG electrodes.

Lastly, the lesion on brain MRI was manually delineated, as used in clinical routine. Recent studies using post-processing MRI analyses based on the classification of surface-based MRI features showed a higher detection rate of FCD than visual inspection, especially useful in patients with negative brain MRI or mild sulcal abnormalities (Ahmed et al., 2015; Thesen et al., 2011). In other words, visual inspection of structural MRI might under-estimates the extent of the FCD network and quantitative post-processing analyses might provide a more exhaustive view of the epileptogenic network. Further studies are necessary to evaluate how quantitative MRI post-processing approaches complement MEG data analysis in order to estimate the full extent of the SOZ in FCD patients.

5. Conclusion

Overall, this study shows that the lesional area, the seizure-onset zone and the MEG spiking volumes in FCD patients are largely co-extensive brain regions but that the SOZ can extend beyond the lesion for some patients. MEG can be viewed as complementary to MRI to estimate the full extent of the SOZ. As a whole, those results highlight the clinical relevance of MEG for the determination of epileptogenic areas in patients with FCD.

Correlation between VIES source power and SEEG Epileptogenicity Index EI: Y: yes N: No/N SEEG contacts: number of SEEG contacts implanted per patient/MEG SV within lesion (%): proportion of the SV determined with VIES included within MRI lesion/lesion within MEG SV: proportion of the MRI lesion included in the MEG SV/Epileptogenic contacts within MEG SV: proportion of highly epileptogenic SEEG contacts (EI > 0.3) included within the MEG SV/Epileptogenic contacts within lesion: proportion of highly epileptogenic SEEG contacts (EI > 0.3) included within the MRI lesion/Epileptogenic contacts within intersection of lesion & SV: proportion of highly epileptogenic SEEG contacts (EI > 0.3) located both within the SV and the MRI lesion/Epileptogenic contacts specific to MEG SV: proportion of highly epileptogenic SEEG contacts (EI > 0.3) included in the MEG SV and outside of the MRI lesion/Epileptogenic contacts specific to lesion: proportion of highly epileptogenic SEEG contacts (EI > 0.3) included in the MRI lesion and outside of the MEG SV.

Funding

Support to this study was provided through grants from the PHRC (Programme Hospitalier de Recherche Clinique) (27-11) 'High Frequency oscillations in Oscillations Magneto-Encephalography (MEG): diagnostic usefulness in presurgical assessment of partial epilepsies', the FFRE (French Foundation for Research on Epilepsy) (FFRE Appel d'Offres Jeune Equipe 2009).

Acknowledgements

Dr. Jung and Dr. Bouet have full access to all the data in the study and take responsibility for the integrity of the data and the accuracy of the data analysis.

None of the authors has any conflict of interest to disclose.

We confirm that we have read the Journal's position on issues involved in ethical publication and affirm that this report is consistent

with those guidelines.

Appendix A. Supplementary data

Supplementary data to this article can be found online at <http://dx.doi.org/10.1016/j.nicl.2017.04.018>.

References

- Agirre-Arrizubieta, Z., Huiskamp, G.J., Ferrier, C.H., et al., 2009. Interictal magnetoencephalography and the irritative zone in the electrocorticogram. *Brain* 132, 3060–3071.
- Ahmed, B., Brodley, C.E., Blackmon, K.E., et al., 2015. Cortical feature analysis and machine learning improves detection of “MRI-negative” focal cortical dysplasia. *Epilepsy Behav.* 48, 21–28.
- Aubert, S., Wendling, F., Regis, J., et al., 2009. Local and remote epileptogenicity in focal cortical dysplasias and neurodevelopmental tumours. *Brain* 132, 3072–3086.
- Avoli, M., Bernasconi, A., Mattia, D., et al., 1999. Epileptiform discharges in the human dysplastic neocortex: in vitro physiology and pharmacology. *Ann. Neurol.* 46, 816–826.
- Bancaud, J., Angelergues, R., Bernouilli, C., et al., 1969. Functional stereotaxic exploration (stereo-electroencephalography) in epilepsies. *Rev. Neurol. (Paris)* 120, 448.
- Bartolomei, F., Chauvel, P., Wendling, F., 2008. Epileptogenicity of brain structures in human temporal lobe epilepsy: a quantified study from intracerebral EEG. *Brain* 131, 1818–1830.
- Bast, T., Oezkan, O., Rona, S., et al., 2004. EEG and MEG source analysis of single and averaged interictal spikes reveals intrinsic epileptogenicity in focal cortical dysplasia. *Epilepsia* 45, 621–631.
- Bast, T., Ramantani, G., Seitz, A., et al., 2006. Focal cortical dysplasia: prevalence, clinical presentation and epilepsy in children and adults. *Acta Neurol. Scand.* 113, 72–81.
- Battal, B., Ince, S., Akgun, V., et al., 2015. Malformations of cortical development: 3T magnetic resonance imaging features. *World J. Radiol.* 7, 329–335.
- Bernasconi, A., Bernasconi, N., Bernhardt, B.C., et al., 2011. Advances in MRI for ‘cryptogenic’ epilepsies. *Nat. Rev. Neurol.* 7, 99–108.
- Blumcke, I., Thom, M., Aronica, E., et al., 2011. The clinicopathologic spectrum of focal cortical dysplasias: a consensus classification proposed by an ad hoc Task Force of the ILAE Diagnostic Methods Commission. *Epilepsia* 52, 158–174.
- Bouet, R., Jung, J., Delpuech, C., et al., 2012. Towards source volume estimation of interictal spikes in focal epilepsy using magnetoencephalography. *NeuroImage* 59, 3955–3966.
- Chassoux, F., Devaux, B., Landre, E., et al., 2000. Stereoelectroencephalography in focal cortical dysplasia: a 3D approach to delineating the dysplastic cortex. *Brain* 123 (Pt 8), 1733–1751.
- Colombo, N., Tassi, L., Deleo, F., et al., 2012. Focal cortical dysplasia type IIa and IIb: MRI aspects in 118 cases proven by histopathology. *Neuroradiology* 54, 1065–1077.
- Engel Jr., J., Rasmussen, T.B., 1993. Outcome With Respect to Epileptic Seizures Surgical Treatment of the Epilepsies. New York, Raven Press, pp. 609–621.
- Englot, D.J., Nagarajan, S.S., Imber, B.S., et al., 2015. Epileptogenic zone localization using magnetoencephalography predicts seizure freedom in epilepsy surgery. *Epilepsia* 56, 949–958.
- Fauser, S., Bast, T., Altenmuller, D.M., et al., 2008. Factors influencing surgical outcome in patients with focal cortical dysplasia. *J. Neurol. Neurosurg. Psychiatry* 79, 103–105.
- Fauser, S., Essang, C., Altenmuller, D.M., et al., 2015. Long-term seizure outcome in 211 patients with focal cortical dysplasia. *Epilepsia* 56, 66–76.
- Ferrer, I., Pineda, M., Tallada, M., et al., 1992. Abnormal local-circuit neurons in epilepsia partialis continua associated with focal cortical dysplasia. *Acta Neuropathol.* 83, 647–652.
- Francione, S., Vigliano, P., Tassi, L., et al., 2003. Surgery for drug resistant partial epilepsy in children with focal cortical dysplasia: anatomical-clinical correlations and neurophysiological data in 10 patients. *J. Neurol. Neurosurg. Psychiatry* 74, 1493–1501.
- Gross, J., Kujala, J., Hamalainen, M., et al., 2001. Dynamic imaging of coherent sources: studying neural interactions in the human brain. *Proc. Natl. Acad. Sci. U. S. A.* 98, 694–699.
- Guerrini, R., Duchowny, M., Jayakar, P., et al., 2015. Diagnostic methods and treatment options for focal cortical dysplasia. *Epilepsia* 56, 1669–1686.
- Hong, S.C., Kang, K.S., Seo, D.W., et al., 2000. Surgical treatment of intractable epilepsy accompanying cortical dysplasia. *J. Neurosurg.* 93, 766–773.
- Ishibashi, H., Simos, P.G., Wheless, J.W., et al., 2002. Localization of ictal and interictal bursting epileptogenic activity in focal cortical dysplasia: agreement of magnetoencephalography and electrocorticography. *Neurol. Res.* 24, 525–530.
- Ishii, R., Canuet, L., Ochi, A., et al., 2008. Spatially filtered magnetoencephalography compared with electrocorticography to identify intrinsically epileptogenic focal cortical dysplasia. *Epilepsy Res.* 81, 228–232.
- Itabashi, H., Jin, K., Iwasaki, M., et al., 2014. Electro- and magneto-encephalographic spike source localization of small focal cortical dysplasia in the dorsal peri-rolandic region. *Clin. Neurophysiol.* 125, 2358–2363.
- Jung, J., Bouet, R., Delpuech, C., et al., 2013. The value of magnetoencephalography for seizure-onset zone localization in magnetic resonance imaging-negative partial epilepsy. *Brain* 136, 3176–3186.
- Knowlton, R.C., Elgavish, R., Howell, J., et al., 2006. Magnetic source imaging versus intracranial electroencephalogram in epilepsy surgery: a prospective study. *Ann. Neurol.* 59, 835–842.
- Lee, S.K., Kim, D.W., 2013. Focal cortical dysplasia and epilepsy surgery. *J. Epilepsy Res.* 3, 43–47.
- Matsumoto, R., Kinoshita, M., Taki, J., et al., 2005. In vivo epileptogenicity of focal cortical dysplasia: a direct cortical paired stimulation study. *Epilepsia* 46, 1744–1749.
- Morioka, T., Nishio, S., Ishibashi, H., et al., 1999. Intrinsic epileptogenicity of focal cortical dysplasia as revealed by magnetoencephalography and electrocorticography. *Epilepsy Res.* 33, 177–187.
- Otsubo, H., Iida, K., Oishi, M., et al., 2005. Neurophysiologic findings of neuronal migration disorders: intrinsic epileptogenicity of focal cortical dysplasia on electroencephalography, electrocorticography, and magnetoencephalography. *J. Child Neurol.* 20, 357–363.
- Palmini, A., Gambardella, A., Andermann, F., et al., 1995. Intrinsic epileptogenicity of human dysplastic cortex as suggested by corticography and surgical results. *Ann. Neurol.* 37, 476–487.
- Rivière, D., Geffroy, D., Dengien, I., et al., 2011. Anatomist: a python framework for interactive 3D visualization of neuroimaging data. In: *Anatomist: A Python Framework for Interactive 3D Visualization of Neuroimaging Data*, (Editor (Ed) (Eds) Book).
- Ryvlin, P., Cross, J.H., Rheims, S., 2014. Epilepsy surgery in children and adults. *Lancet Neurol.* 13, 1114–1126.
- Tassi, L., Pasquier, B., Minotti, L., et al., 2001. Cortical dysplasia: electroclinical, imaging, and neuropathologic study of 13 patients. *Epilepsia* 42, 1112–1123.
- Thesen, T., Quinn, B.T., Carlson, C., et al., 2011. Detection of epileptogenic cortical malformations with surface-based MRI morphometry. *PLoS One* 6, e16430.
- Varotto, G., Tassi, L., Franceschetti, S., et al., 2012. Epileptogenic networks of type II focal cortical dysplasia: a stereo-EEG study. *NeuroImage* 61, 591–598.
- Wang, Z.I., Alexopoulos, A.V., Jones, S.E., et al., 2014. Linking MRI postprocessing with magnetic source imaging in MRI-negative epilepsy. *Ann. Neurol.* 75, 759–770.
- Widdess-Walsh, P., Jeha, L., Nair, D., et al., 2007. Subdural electrode analysis in focal cortical dysplasia: predictors of surgical outcome. *Neurology* 69, 660–667.
- Widjaja, E., Otsubo, H., Raybaud, C., et al., 2008. Characteristics of MEG and MRI between Taylor’s focal cortical dysplasia (type II) and other cortical dysplasia: surgical outcome after complete resection of MEG spike source and MR lesion in pediatric cortical dysplasia. *Epilepsy Res.* 82, 147–155.
- Wilenius, J., Medvedovsky, M., Gaily, E., et al., 2013. Interictal MEG reveals focal cortical dysplasias: special focus on patients with no visible MRI lesions. *Epilepsy Res.* 105, 337–348.